



ARCHIVES
of
FOUNDRY ENGINEERING

ISSN (2299-2944)
Volume 2022
Issue 3/2022

41 – 52





10.24425/afe.2022.140235

6/3



Published quarterly as the organ of the Foundry Commission of the Polish Academy of Sciences

Modelling of Plastic Flow Behaviour of Metals in the Hot Deformation Process Using Artificial Intelligence Methods

B. Mrzygłód * , A. Łukaszek-Solek , I. Olejarczyk-Woźeńska , K. Pasierbiewicz 
AGH University of Science and Technology, Faculty of Metals Engineering and Industrial Computer Science,
Cracow, Poland

* Corresponding author. E-mail address: mrzyglod@agh.edu.pl

Received 17.03.2022; accepted in revised form 17.05.2022; available online 07.09.2022

Abstract

Hot deformation of metals is a widely used process to produce end products with the desired geometry and required mechanical properties. To properly design the hot forming process, it is necessary to examine how the tested material behaves during hot deformation. Model studies carried out to characterize the behaviour of materials in the hot deformation process can be roughly divided into physical and mathematical simulation techniques.

The methodology proposed in this study highlights the possibility of creating rheological models for selected materials using methods of artificial intelligence, such as neuro-fuzzy systems. The main goal of the study is to examine the selected method of artificial intelligence to know how far it is possible to use this method in the development of a predictive model describing the flow of metals in the process of hot deformation.

The test material was Inconel 718 alloy, which belongs to the family of austenitic nickel-based superalloys characterized by exceptionally high mechanical properties, physicochemical properties and creep resistance. This alloy is hardly deformable and requires proper understanding of the constitutive behaviour of the material under process conditions to directly enable the optimization of deformability and, indirectly, the development of effective shaping technologies that can guarantee obtaining products with the required microstructure and desired final mechanical properties.

To be able to predict the behaviour of the material under non-experimentally tested conditions, a rheological model was developed using the selected method of artificial intelligence, i.e. the Adaptive Neuro-Fuzzy Inference System (ANFIS).

The source data used in these studies comes from a material experiment involving compression of the tested alloy on a Gleeble 3800 thermo-mechanical simulator at temperatures of 900, 1000, 1050, 1100, 1150°C with the strain rates of 0.01 - 100 s⁻¹ to a constant true strain value of 0.9.

To assess the ability of the developed model to describe the behaviour of the examined alloy during hot deformation, the values of yield stress determined by the developed model (ANFIS) were compared with the results obtained experimentally. The obtained results may also support the numerical modelling of stress-strain curves.

Keywords: Adaptive neuro-fuzzy inference system, Rheological model, Inconel 718, Hot deformation



1. Introduction

Hot deformation of metals is a widely used process to produce end products with the desired geometry and required properties. To properly design this process, it is necessary to study the material behaviour during hot deformation. The values of the flow stress during hot deformation of materials depend on many factors, including strain, strain rate, temperature, etc. The phenomena that occur during this process are usually non-linear and therefore difficult to model.

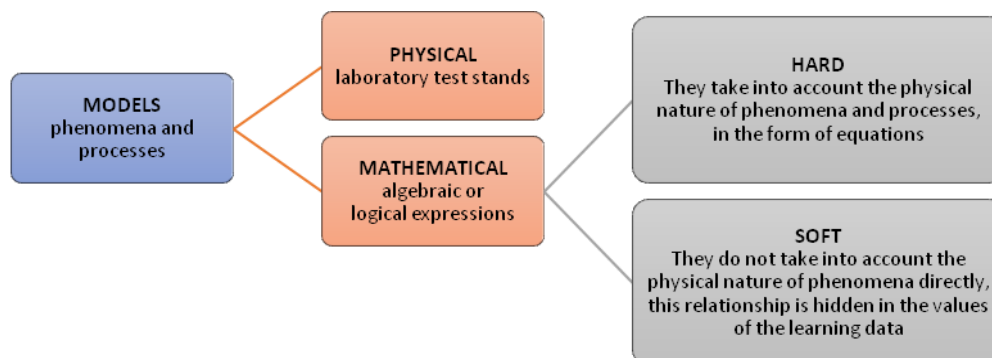


Fig. 1. The basic criterion for the division of methods used in phenomena modelling [1]

Physical modelling involves the design of special test stands, where the controlled conditions of the process are simulated and process behaviour is observed (e.g. Gleeble apparatus).

The second group is **mathematical modelling**, which describes in the form of appropriate mathematical expressions the cause-and-effect relationships occurring in the process. The most popular in this field is **hard modelling** which takes into account the physical nature of the discussed phenomena and processes, formalized in the form of algebraic expressions which, apart from numbers, usually also include variables and numerical parameters. The primary techniques using this approach are all CAx systems. In programs based on the finite element method (FEM), the effectiveness of numerical simulation of the material shaping process is strongly dependent on the accuracy of the models used, including a detailed explanation/description of flow stress as a function of strain, strain rate and temperature, considered to be the key factor determining the dynamic response/reaction of material to the application of a specific combination of thermo-mechanical process conditions [2]. The yield stress depends on the material parameters, and these in turn depend on the deformation history, strain rate and temperature. Therefore, a whole range of constitutive models describing the behaviour of the tested material during deformation, including hot deformation, has been developed and used in practice [3-5].

The non-linear nature of the material response to changes in process parameters makes an accurate description of the material flow very difficult. The constitutive models describing the behaviour of materials during deformation can be divided into the following characteristic groups [6]:

- **Phenomenological models** – these models are based on matching experimental data to appropriate mathematical equations/functions and define plastic flow stress as a function of temperature, strain rate and strain. They are

1.1. Methods of modelling the behaviour of metals during hot deformation

Modelling studies to characterize the behaviour of metals during hot deformation can be roughly divided into physical and mathematical simulation techniques (Fig. 1).

widely used for various types of metals and their alloys, do not require detailed understanding of physical phenomena involved in the deformation process, use regression analysis to reduce the number of material constants describing the constitutive relationship between stress and process variables, and can be easily calibrated. These can be classical or modified models, e.g. Johnson-Cook (JC) model [7-9], Arrhenius equation, Molinari-Ravichandran (MR) model [10].

- **Physical models** – these models take into account physical aspects of material deformation, are based on the theory of thermodynamics, thermally activated dislocation motion and slip kinetics. They are obtained by fitting and regression of experimental data and are based on a large number of material constants, the determination of which requires high-accuracy instruments used during the hot and dynamic deformation process when the internal microstructure of the tested material undergoes significant changes. In cases where phenomenological models are unable to provide an accurate interpretation, physical models take into account e.g. the dislocation evolution mechanism or the energy of thermal activation, but complexity limits their application in commercially used finite element softwares (FEM). Examples of classical and modified physical models include Zerilli-Armstrong (ZA) model [11-12]; dynamic recrystallization (DRX) model [13]; cellular automaton (CA) model [14].

Soft modelling is a special group of methods which, contrary to hard modelling, does not take into account the physical nature of phenomena but detect the cause-and-effect relationships occurring in the analysed process through a special analysis of the obtained source data. This group of methods assumes that all knowledge

about the process is hidden in the values of the obtained experimental data constituting the direct basis for modelling. This modelling uses the most popular methods in the field of artificial intelligence, namely:

- Artificial neural networks (ANNs) and adaptive neuro-fuzzy inference system (ANFIS) - known as universal approximators of functions, useful mainly when it is necessary to model phenomena of a strongly non-linear nature and multi-dimensional functional relationships, which are difficult to determine in a purely analytical form. These methods perfectly cope with uncertain and incomplete source data, and uncertainty and incompleteness are the predominant features of the source data obtained from experiments [15-17]. The source data obtained from experiments is valid only for selected cases, and so it is incomplete, it is additionally burdened with measurement errors, and so it is uncertain. This group of methods has gained particular popularity as a tool for building models which describe the behaviour of material during deformation as a function of high temperature and strain rate. The relationship is non-linear but numerous factors that control flow stress are also non-linear, and this allows predicting the value of flow stress with much higher accuracy than the accuracy provided by regression methods. One of the main advantages of this approach is that it is not necessary to postulate a mathematical model or identify its parameters using regression methods. Literature describes various cases when this approach has been used to determine rheological models [18-24]. The authors of models [18-21] have demonstrated that the accuracy of the ANN fit with regard to the flow stress in alloys of Pb-Mg-10Al-0.5B [19] and Ti-6Al-4V [20] is much better than the accuracy obtained when constitutive equations are used. While ANNs are used to model the flow curves for various types of alloys, studies using ANFIS can be found only for a few alloys, like Sn-5Sb [23], Ti60 [24], 6063 aluminium alloy [25], Ti600 [26], Ni-based superalloy [27].

1.2. Constitutive modelling of the Inconel 718 alloy

Among the models used to simulate the behaviour of materials during hot deformation, there are phenomenological constitutive models.

The literature describes numerous studies carried out on the Inconel 718 alloy. Inconel 718 is a hardly deformable alloy that requires high forming temperatures and narrow ranges of other process parameters. At the same time it is one of the most widely studied nickel-based alloys which, owing to their wide application,

are still interesting to many researchers. As a nickel-based, precipitation-hardened superalloy, wrought Inconel 718 is mainly used for gas turbine rotors, rocket engines, nuclear reactor components, pumps and instrumentation.

One of the most popular approaches to studies of the Inconel 718 alloy involves the use of Arrhenius constitutive equations. They express the flow stress in the form of a mathematical equation where material constants can be determined by the regression analysis based on experimental results. Unfortunately, the traditional Arrhenius equation does not take into account the effect of strain on the value of flow stress which, as is generally known, is important because the stress-strain curves are representative of the process of strain hardening or dynamic softening. After the first application by Jonas [28], this model was modified to obtain more accurate and precisely predicted stress values by assuming that constants in the model depend on the strain value [29-30]. This requires the use of multiple regression, calculation of material constants for each value of deformation and matching the optimal degree of polynomial. Another popular method used to test the Inconel 718 alloy is the Johnson-Cook method and its developments, e.g. Johnson-Cook and Zerilli-Armstrong (JC-ZA) method. This model was tested for its ability to predict the flow stress in materials, assessed through the correlation coefficient, mean absolute error and its standard deviation [31].

Despite wide interest in this type of models, some of their disadvantages can be indicated, like mathematical formulation necessary for the algorithmic transformation of input data into output data, low accuracy of the regression method when predicting the non-linear relationships between stress and process variables, especially for high values of the strain rate, the need to recalculate constants in the case of adding new experimental data, and time-consuming procedures [18, 26, 32].

There are examples in the literature of the use of soft modelling for Inconel 718 alloys [33-34], but these methods are mainly used to study the alloy physical properties other than the properties discussed in this article [35].

2. Research methodology

The aim of this study is to present the selected research methodology and the results obtained in the development of a rheological model for the Inconel 718 alloy using an ANFIS algorithm. A diagram of the adopted research methodology is shown in Figure 2. The research includes the following stages: an experiment carried out on the selected test material, collecting the obtained experimental source data, selecting a modelling method and determining model parameters, and analysis of hardening curves generated by the developed model.

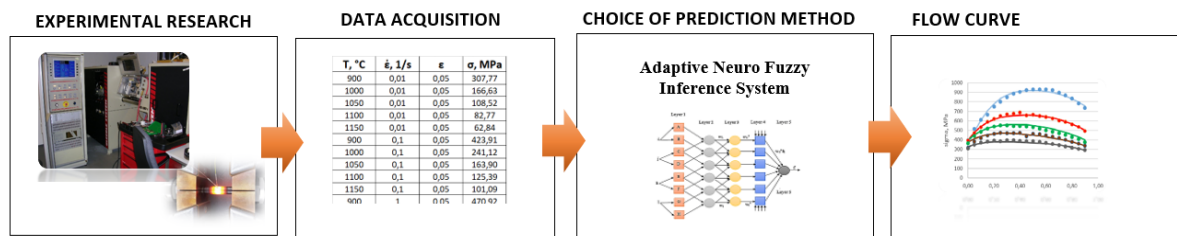


Fig. 2. Scheme of research methodology used for the construction of rheological models

2.1. Test material and experimental procedure

The source data used in these studies comes from a material experiment involving a compression test carried out on the alloy delivered in the form of a 50 mm diameter rod. The chemical composition of the alloy tested is shown in Table 1.

Table 1.

Chemical composition (wt%) of the tested Inconel 718 alloy

Al	Co	Fe	C	Mo	Cr	Ti	Nb	Ni
0,49	0,20	18,12	0,024	2,90	17,95	1,00	5,22	rest

The original microstructure of Inconel 718 alloy is shown in Fig. 3. On delivery within the alloy investigated there are: phase separation δ (needle-shaped precipitates within the grains boundaries), NbC and TiC carbides in the matrix of the fcc crystal structure. This proves that the material as delivered has not been fully heat treated by the manufacturer.

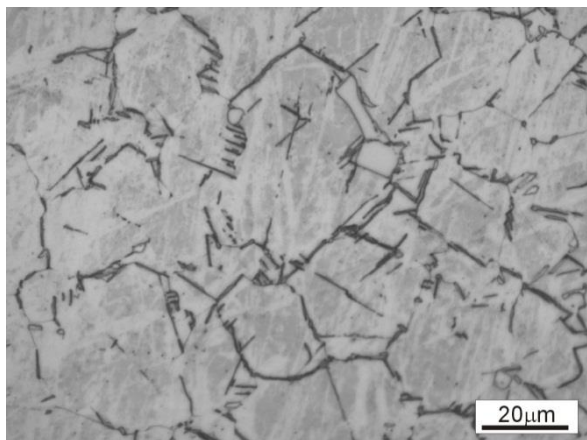


Fig. 3. The original microstructure of Inconel 718 alloy

The tests were carried out using a Gleeble 3800 thermo-mechanical simulator (Fig. 4) operating in a protective argon atmosphere. Through upsetting, the samples in the simulator were undergoing a true strain of 0.9. The heating rate was 2.5°C/s, the holding time was 10 s. After deformation, the samples were cooled in a jet of compressed air.



Fig. 4. Gleeble 3800 thermo-mechanical simulator

Axial-symmetric samples with dimensions of $\varnothing 10 \times 12$ mm taken from the alloy were subjected to a compression test carried out at 900, 1000, 1050, 1100, 1150 [°C] with average strain rates equal to 0.01; 0.1; 1; 10; 100 [s^{-1}]. The ranges of parameter values used in the compression test were taken from the literature. However, considering the lack of data on the behaviour of nickel alloys during deformation at high strain rates, despite problems with the precise control of parameters, tests were also carried out for the strain rate of 100 s^{-1} . It was thought that the results might prove useful when designing the forming processes for high-speed machines.

2.2. Source data acquired

As a result of the studies, a database of experimental results containing 475 knowledge records was created. The input data included temperature, strain and strain rate. The output data (the dependent variable) was the stress value measured under given process conditions. The ranges of the values of the tested parameters are summarized in Table 2, while Table 3 shows a fragment of the developed database.

Table 2.

List and ranges of the analysed input parameters

Parameters		Ranges	
		Min.	Max.
INPUTS			
Temperature	T, °C	900	1150
Strain	$\dot{\epsilon}$, 1/s	0,01	100
Strain rate	ϵ	0	0,9
OUTPUT			
Stress	σ , MPa	52,342	931,343

Table 3.

Fragment of the acquired experimental data

T, °C	$\dot{\epsilon}$, 1/s	E	σ , MPa
900	0,01	0,00	248,906
1000	0,01	0,00	136,706
1050	0,01	0,00	87,944
1100	0,01	0,00	67,512
1150	0,01	0,00	52,342
900	0,1	0,00	309,446
1000	0,1	0,00	196,492
1050	0,1	0,00	136,093
1100	0,1	0,00	111,226
1150	0,1	0,00	90,845
900	1	0,00	335,036
1000	1	0,00	291,715
1050	1	0,00	224,541
1100	1	0,00	175,104
1150	1	0,00	149,092
900	10	0,00	342,686
1000	10	0,00	280,424
1050	10	0,00	313,916
1100	10	0,00	261,074
1150	10	0,00	210,558
900	100	0,00	395,462
1000	100	0,00	392,053
1050	100	0,00	365,436
1100	100	0,00	317,121
1150	100	0,00	309,871
900	0,01	0,05	307,769
...

Based on the ANFIS algorithm, the data collected in the table was used to develop a predictive model simulating the behaviour of the tested material under non-experimentally tested conditions.

2.3. Adaptive Neuro-Fuzzy Inference System

Fuzzy systems have attracted a lot of attention in recent years. First of all, they require much less information to model various

phenomena than the classical modelling methods, and secondly, they are very good at processing uncertain and incomplete information. In fuzzy logic, the knowledge about the problem is written in the form of rules. In the presented study, a fuzzy Sugeno-type inference system [36] was selected for fuzzy inference, the rules of which are characterized by premises written in the form of fuzzy sets, while conclusions are determined in the form of linear relationships (1).

$$\text{If } x \text{ is } A \text{ and } y \text{ is } B \text{ then } z_I = a_I x + b_I y + c_I \quad (1)$$

where:

- x and y – explanatory (input) variables,
- A, B – names of fuzzy sets representing premises,
- z_I – the dependent (output) variable, the value of which is represented by a linear functional relationship,
- a_I, b_I, c_I – coefficients in the linear description of the function.

Figure 5 is an example of the inference system mapping four rules, the conclusions of which are linear functions operating in a narrow range of specific fuzzy sets. An appropriate inference mechanism adopted for the Sugeno system can provide a smooth transition from one linear function to another for areas where the sets overlap. As a result, based on the Sugeno model, it is possible to build a fuzzy system that switches between several local linear solutions acting as a strongly non-linear system that moves globally around its operating point.

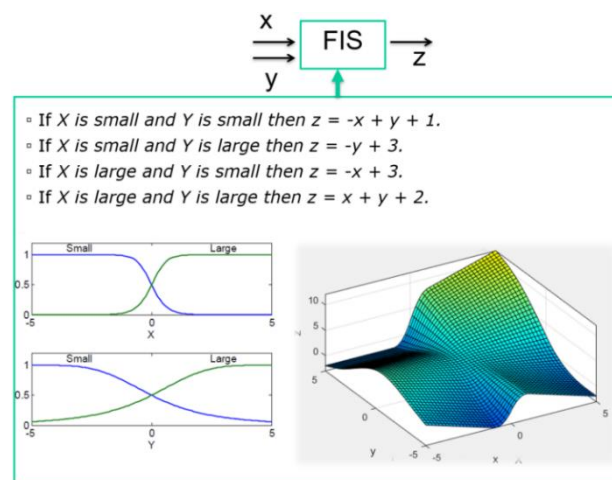


Fig. 5. An example of the Sugeno inference system

Fuzzy inference system (FIS) structure identification includes:

- determining input and output variables,
 - dividing the ranges of input variables into an appropriate number of fuzzy sets with a specific shape of the membership function,
 - parametric identification and estimation of parameters of the membership function of fuzzy sets of inputs,
 - parametric identification of parameters of the linear models appearing in the conclusions of the rules,
- determining fuzzy rules of the IF-THEN type interrelating fuzzy premises with linear conclusions. Each rule represents

one narrow local system of dependencies occurring in the analysed process.

Adaptive Neuro-Fuzzy Inference System (ANFIS) [37] is a hybrid algorithm which, using available training data, determines the optimal FIS parameters, i.e.:

- parameters of the membership function of fuzzy sets for input variables,
- coefficients of linear functions appearing in the conclusions of the rules,
- a set of fuzzy rules of the IF-THEN type.

The process of determining the parameters of the FIS system is carried out by constantly changing these parameters as a result of

presenting the system with individual model cases from the training sample. Training is iterative and consists in:

- tuning parameters of the membership function of fuzzy sets occurring in the premises of the rules - this operation is based on the error back propagation algorithm,
- updating the coefficients of linear functions appearing in the conclusions of the rules - this operation is performed by the least squares method.

The general scheme of data processing in the ANFIS algorithm consists of several computational layers, which are schematically presented in Figure 6.

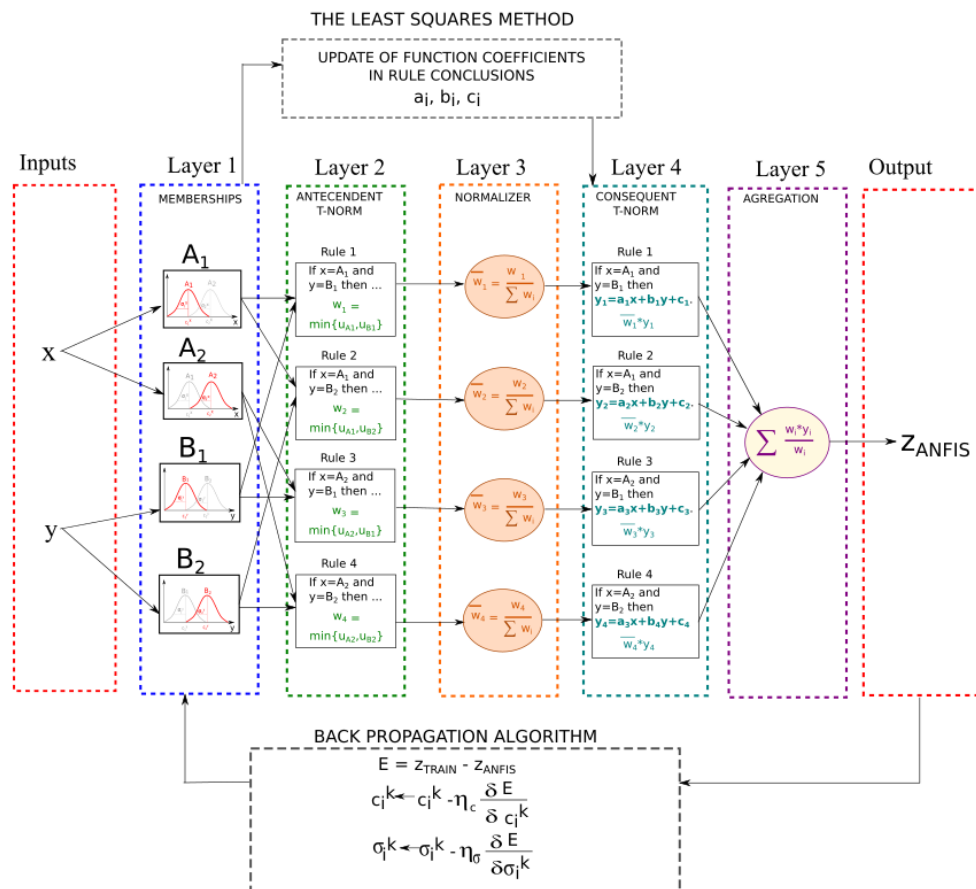


Fig. 6 Architecture of the ANFIS algorithm

The initial layer (INPUTS) is responsible for the transfer of input variables from the training set (x_1, x_2, \dots, x_n), and the first layer (L1) performs the fuzzification process, i.e. determining the coefficients of the membership of each input vector x_i in the adopted fuzzy sets A_i^k of each variable. The second layer (L2) determines the degree of activation of the premises of the k -th rule w_k . The elements of this layer follow the t-norm, e.g. in the form of the product. The obtained value is normalized in the next layer (L3). The fourth layer (L4) computes the conclusion values of the k -th rule y_k , which are then weighted by the degrees of the truth of the logical rules (w_i). In the fifth layer (L5) they are added together.

The output gives the predicted value of the dependent variable for the modelled sample. Here, the output from the model is compared with the pattern in the training data, the error is calculated based on the difference between the calculated response of the i -th FIS and the pattern response obtained for this case, and information about the error is sent to the previous layer and FIS parameters are modified in accordance with the adopted principle. The ANFIS model uses hybrid training, i.e. gradient training combined with least squares estimation.

- Step 1 - the parameters of the premises (fuzzy sets) are constant - construction of local linear models: the parameters

of the rule conclusions are determined (least squares estimation).

- Step 2 – the parameters of the rule conclusions are constant (coefficients of linear functions). The error is calculated and then propagated backwards. The parameters of the rule conditions (parameters of the membership function of fuzzy sets) are modified with partial derivatives of the error function (gradient training).

The training is stopped when the average error has reached the assumed minimum.

3. Results and discussion

3.1. Experimental stress-strain behaviour

The true stress-strain curves of Inconel 718 at temperatures from 900°C to 1150°C and the strain rates ranging from 0.01 to 100 s⁻¹ up to a true strain of 0,9 are shown in Fig. 7.

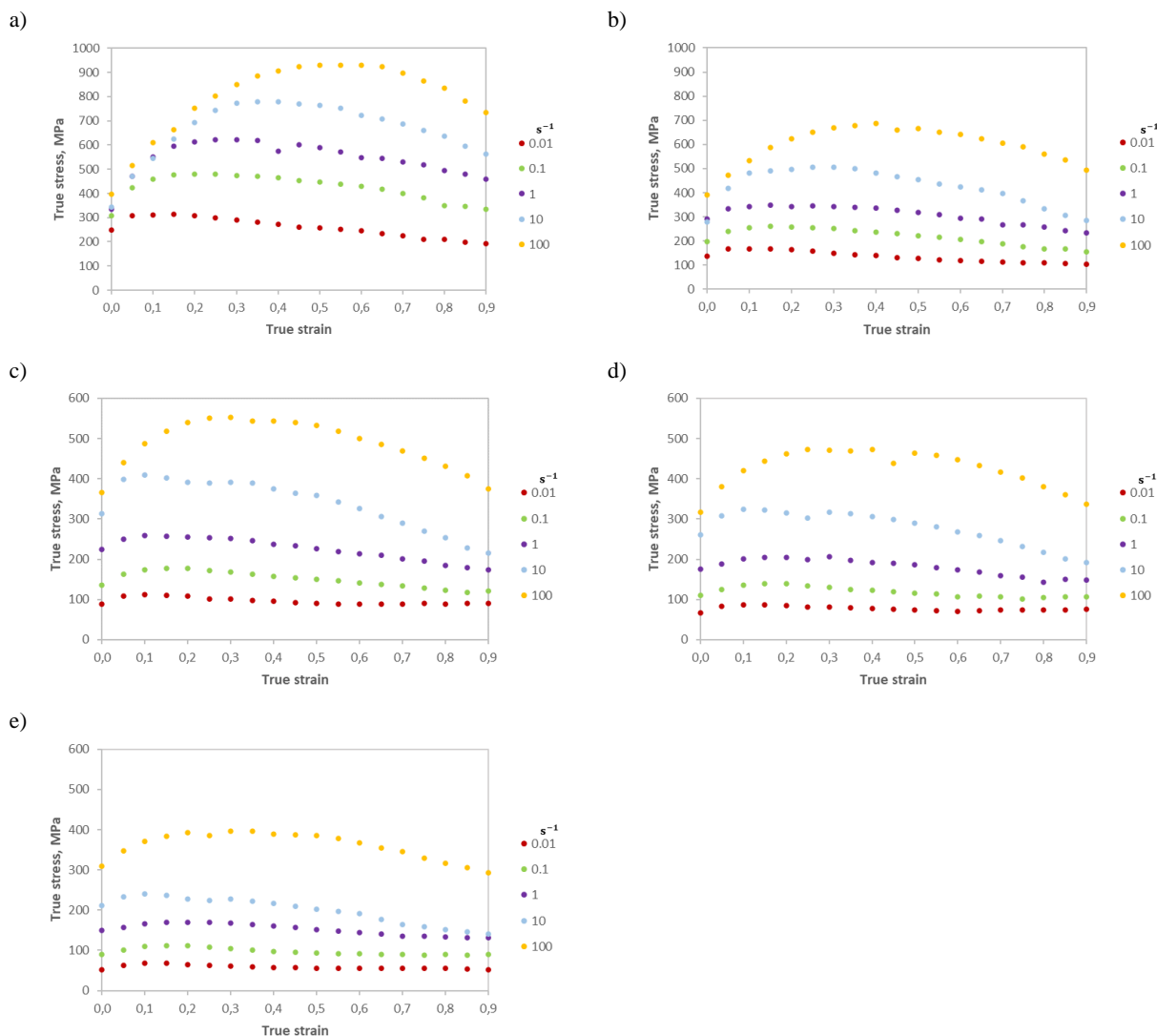


Fig. 7. The stress – strain curves of Inconel 718: a) at 900°C for different strain rates, b) at 1000°C for different strain rates, c) at 1050°C for different strain rates, d) at 1100°C for different strain rates, e) at 1150°C for different strain rates

It is easy to note that the stress-strain curves slightly differ in shape depending on the strain rate and temperature. The stress increases with the increase in strain rate and decreases in

temperature, thus suggesting that during hot compression the stress is sensitive to both strain rate and temperature. The main reason for the increase in stress value with the increase in strain rate may be

the energy accumulation time, the lower is the strain rate, the longer is the time. High temperature and lower strain rates promote a longer time for the nucleation process and the growth of dynamically recrystallized grains as well as the annihilation of dislocations, thus reducing the stress level [38]. Additionally, the flow stress increases at the beginning of the deformation process. It is related to the rate of material hardening caused by the rapid generation and multiplication of dislocations [39]. The intensive process of material hardening in the initial phase is visible at temperatures below 1150°C. At the same time, the dynamic recovery associated with the climbing and sliding of dislocations is too weak to overcome the hardening effect. As the true strain increases, the flow stress also increases to its maximum (peak) value, to undergo later a gradual decrease. The softening of the tested material, manifested by a decrease in true stress after exceeding the maximum value with the strain increase, may be the result of a recrystallization process and dynamic recovery of material, or instability of material flow [40-41]. A steady course of the curves was observed for lower strain rates.

3.2. Fuzzy FIS model developed using ANFIS

Three input variables were adopted as an input to the algorithm, i.e. temperature, strain and strain rate. Stress was adopted as an output. A schematic diagram of the FIS model with input and output variables is shown in Figure 8.

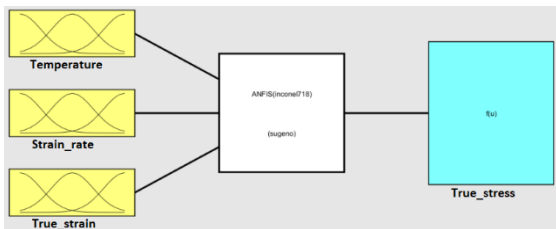


Fig. 8. Schematic diagram of the FIS model with input and output variables

In the training process, tests were carried out on many FIS architectures with the different numbers of the fuzzy sets for input variables and types (shapes) of membership functions. The best results were obtained for the structure where all fuzzy sets of input variables were Gaussian in nature. The adopted formula is presented in equation (2), and its graphical form is presented in Figure 9.

$$\mu_A(x; \bar{x}; \sigma) = \exp\left(-\left(\frac{x - \bar{x}}{\sigma}\right)^2\right) \quad (2)$$

where: \bar{x} - centre, σ - width of the fuzzy set.

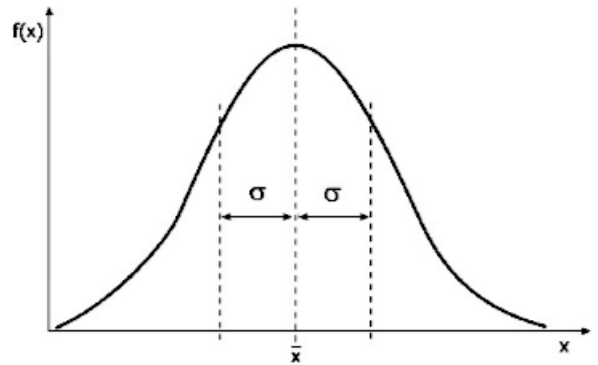


Fig. 9. Graphical representation of the Gaussian membership function

The temperature and strain rate variables were divided into five fuzzy sets, while the strain variable was divided into three fuzzy sets. The structure of the developed ANFIS model is presented in Figure 10.

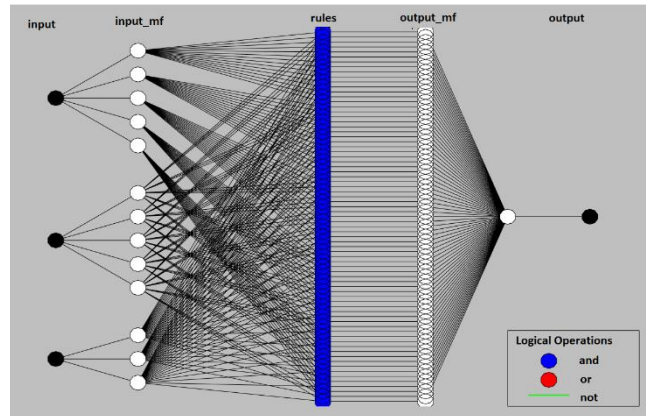


Fig. 10. The structure of the ANFIS model developed to predict stress values

The model comprised 75 generated subspaces, where each of the subspaces was represented by one fuzzy rule describing system operation in this subspace. The general form of the rules is presented in formula (3).

$$\text{IF } (x_1 = A_1) \text{ and } (x_2 = B_2) \text{ and } (x_3 = C_3) \quad (3)$$

$$\text{THEN } y_1 = f_1(x_1, x_2, x_3)$$

The simulation performed with the designed algorithm gave very satisfactory results. The minimum training RMSE determined by the formula (4) was achieved as early as in the 23rd epoch and was at a level of 3.328 (Fig. 11a). Figure 11b compares calculations derived from the FIS model with training data.

$$RMSE = \sqrt{\frac{1}{n} \sum_{i=1}^n (y_i - \bar{y}_i)^2} \quad (4)$$

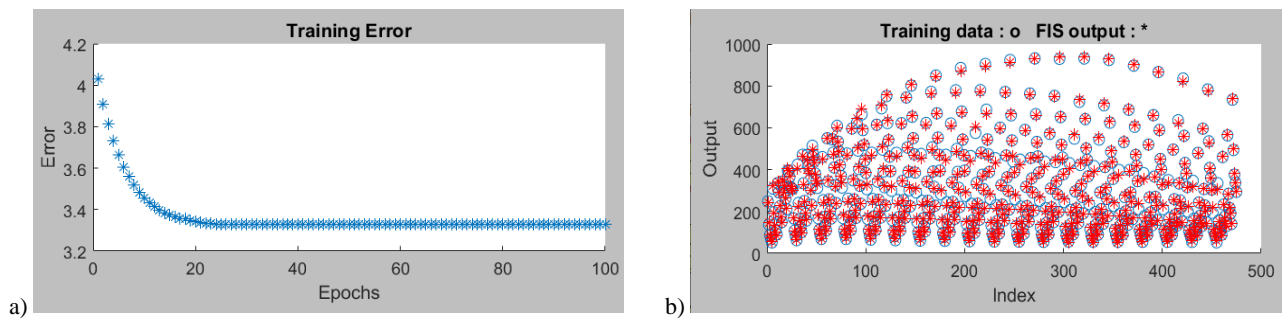


Fig. 11. Outcomes of the training process: a) the course of the training error, b) training data compared with the results of modelling

Figure 12 shows graphical representation of fuzzy sets determined by ANFIS in the training process for the adopted input variables, i.e.: (a) temperature, (b) strain, (c) strain rate.

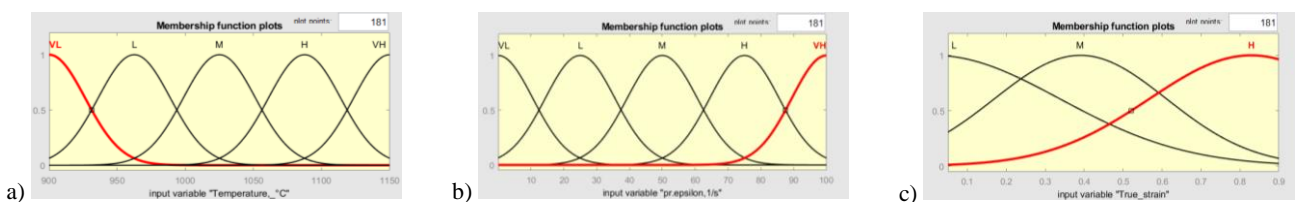


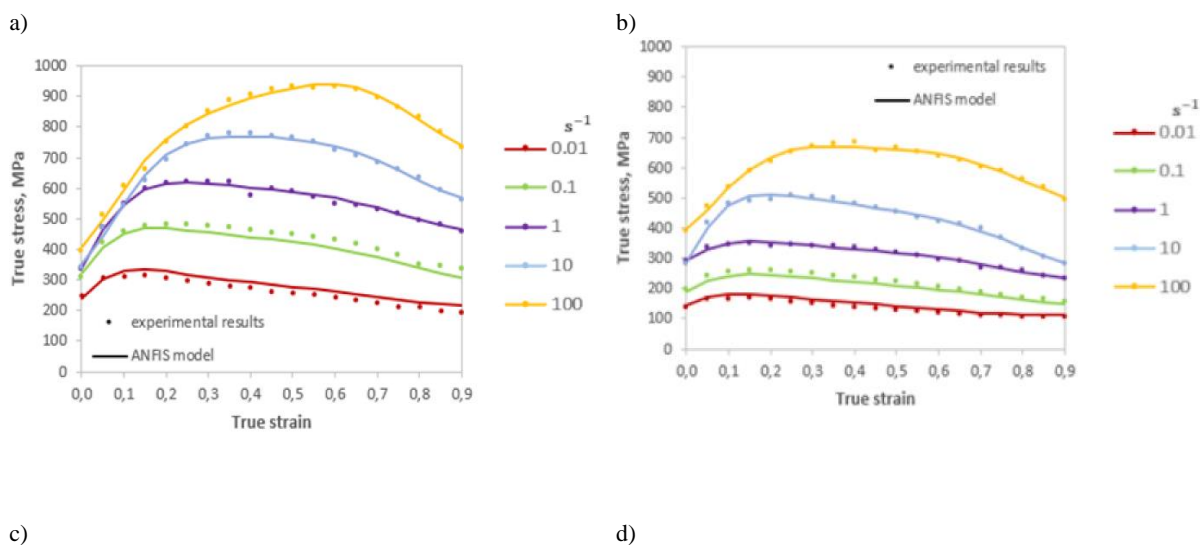
Fig. 12. Graphical representation of the input variables: a) temperature, b) strain rate, c) strain

3.3. Adaptive Neuro-Fuzzy Inference System

The results obtained on the developed predictive model simulating the behaviour of Inconel 718 under the non-experimentally tested conditions are discussed. Figure 13 shows comparative plots obtained for the experimental results (dotted line) and values predicted by ANFIS model (solid line) at (a) 900 °C, (b) 1000 °C, (c) 1050 °C and (d) 1100 °C, (e) 1150 °C.

A comparison of the experimental flow curves with the curves predicted by ANFIS model for the same temperature parameters,

i.e. from 900 to 1150°C, and strain rates, i.e. from 0.01 to 100 s⁻¹, showed a similar course of the curves in the full range of deformation values. Hence it can be concluded that in the entire process space the calculated values of stress show very high goodness of fit with the experimental data. This indicates the correct selection of the stress prediction model for the examined range of the temperature and strain rate values and indicates that the developed model can be used to predict the values of stress in the examined nickel alloy.



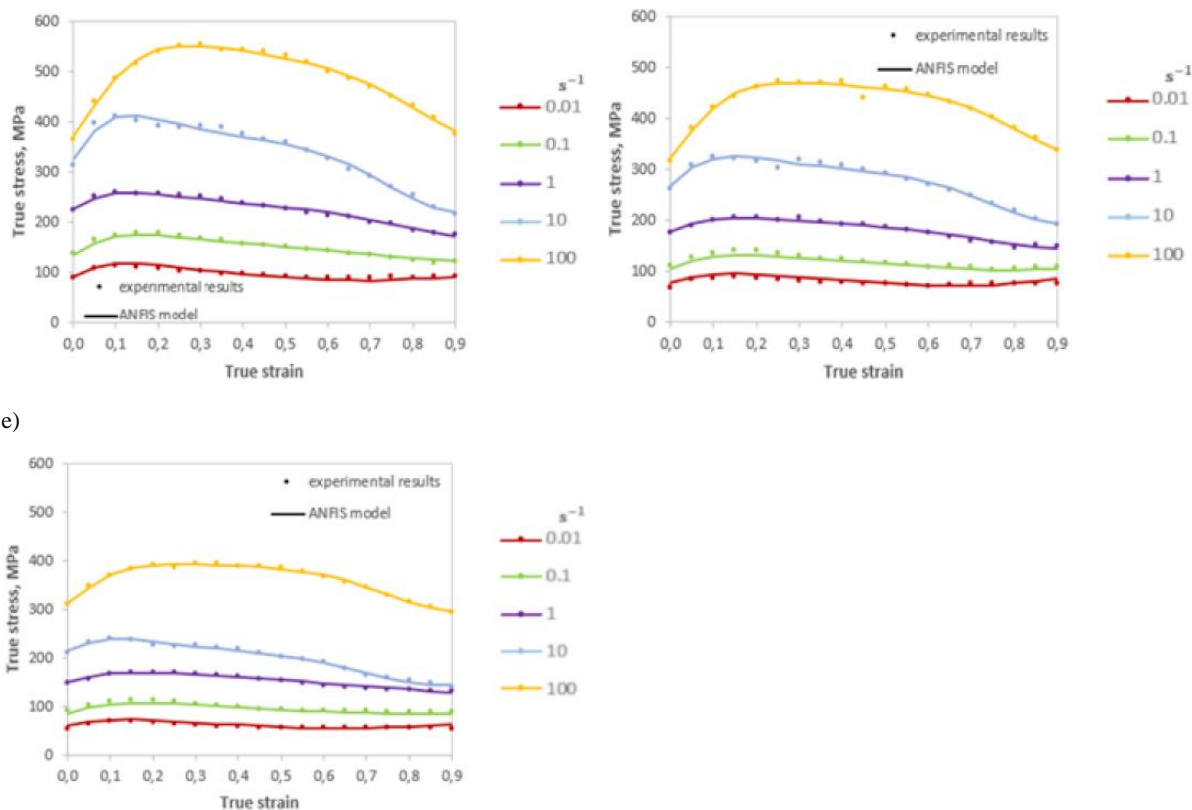


Fig. 13 Comparative plots of the experimental results (solid line) and values predicted by ANFIS model (dotted line) at (a) 900°C, (b) 1000°C, (c) 1050°C and (d) 1100°C, (e) 1150°C

4. Summary

Modelling of the Inconel 718 alloy plastic flow behaviour in a hot deformation process using artificial intelligence methods was described. Source data from the material experiment, which comprised the compression test in a Gleeble thermo-mechanical simulator carried out at temperatures of 900, 1000, 1050, 1100, 1150 [°C] and strain rates of 0.01; 0.1; 1; 10; 100 [s⁻¹], was used in the research.

The following conclusions can be derived from this study:

- An analysis of the flow curves was performed and it was found that with the increasing value of true strain, the flow stress was also increasing to its maximum (peak) value, to decrease gradually later on.
- The flow curves were plotted since the literature provides no information on the use of the neuro-fuzzy ANFIS algorithm to develop the flow curves for the tested nickel alloy. For the entire range of temperature values, i.e. 900 - 1150°C, and the strain rates of 0.01 - 100 s⁻¹, a high degree of compliance was obtained between stress values determined by the model and experimental data.
- The developed flow curves can be used for numerical modelling of the plastic forming process of Inconel 718 alloy.

Acknowledgements

The research project was financed by the Ministry of Education and Science (AGH-UST statutory research project no. 16.16.110.663).

References

- [1] Grzegorzewski, P., A. Kochański, A. (2019). *Data and modeling in industrial manufacturing*. In: Grzegorzewski, P., Kochanski, A., Kacprzyk, J. (eds) *Soft Modeling in Industrial Manufacturing*. Studies in Systems, Decision and Control, 183. Springer, Cham. DOI:10.1007/978-3-030-03201-2_1
- [2] Bobbili, R., Venkata, R. & Madhu, V. (2017). A physically-based constitutive model for hot deformation of Ti-10-2-3 alloy. *Journal of Alloys and Compounds*. 696, 295-303. <https://doi.org/10.1016/j.jallcom.2016.11.208>
- [3] Gronostajski, Z. (2000). The constitutive equations for FEM analysis. *Journal of Materials Processing Technology*. 106(1-3), 40-44. DOI:10.1016/S0924-0136(00)00635-X
- [4] Luo, J., Li, M., Li, X. & Shi, Y. (2010). Constitutive model for high temperature deformation of titanium alloys using

- internal state variables. *Mechanics of Materials*. 42(2), 157-165. DOI:10.1016/j.mechmat.2009.10.004
- [5] Voyiadjis, G.Z. & Abed, F.H. (2005). Microstructural based models for bcc and fcc metals with temperature and strain rate dependency. *Mechanics of Materials*. 37(2-3), 355-378. DOI: 10.1016/j.mechmat.2004.02.003
- [6] Lin, Y. & Xiao-Min, C. (2011). A critical review of experimental results and constitutive descriptions for metals and alloys in hot working. *Materials and Design*. 32(4), 1733-1759. DOI:10.1016/j.matdes.2010.11.048
- [7] Johnson, G. & Cook, W. (1985). Fracture characteristics of three metals subjected to various strains, strain rates, temperatures and pressures. *Engineering Fracture Mechanics*. 21(1), 31-48. [https://doi.org/10.1016/0013-7944\(85\)90052-9](https://doi.org/10.1016/0013-7944(85)90052-9)
- [8] Zhang, H., Wen, W. & Cui, H. (2009). Behaviors of IC10 alloy over a wide range of strain rates and temperatures. experiments and modeling. *Materials Science and Engineering A*. 504(1-2), 99-103. DOI:10.1016/j.msea.2008.10.056
- [9] Lin, Y., Chen, X. & Liu, G. (2010). A modified Johnson-Cook model for tensile behaviors of typical high-strength alloy steel. *Materials Science and Engineering A*. 527(26), 6980-6986. DOI:10.1016/j.msea.2010.07.061
- [10] Molinaria, A. & Ravichandran, G. (2005). Constitutive modeling of high-strain-rate deformation in metals based on the evolution of an effective microstructural length. *Mechanics of Materials*. 37(7), 737-752. DOI: 10.1016/j.mechmat.2004.07.005
- [11] Zerilli, P. & Armstrong, R. (1987). Dislocation-mechanics-based constitutive relations for material dynamics calculations. *Journal of Applied Physics*. 61, 1816-1825. <https://doi.org/10.1063/1.338024>
- [12] Samantaray, D., Mandal, S., Borah, U. & Bhaduri, A. (2009). A thermo-viscoplastic constitutive model to predict elevated-temperature flow behaviour in a titanium-modified austenitic stainless steel. *Materials Science and Engineering A*. 526(1-2), 1-6. DOI:10.1016/j.msea.2009.08.009
- [13] Lin, Y., Chen, M. & Zhang, J. (2008). Prediction of 42CrMo steel flow stress at high temperature and strain rate. *Mechanics Research Communications*. 35(3), 142-50. DOI:10.1016/j.mechrescom.2007.10.002
- [14] Goetz, R. & Seetharaman, V. (1998). Modeling dynamic recrystallization using cellular automaton. *Scripta Materialia*. 38(3), 405-13. DOI: 10.1016/s1359-6462(97)00500-9
- [15] Hawryluk, M. & Mrzygłód, B. (2018). A system of analysis and prediction of the loss of forging tool material applying artificial neural networks. *Journal of Mining and Metallurgy. Section: B, Metallurgy*. 54(3), 323-337. <https://doi.org/10.2298/JMMB180417023H>
- [16] Mrzygłód, B., Gumienny, G., Wilk-Kołodziejczyk, D. & Regulski, K. (2019). Application of selected artificial intelligence methods in a system predicting the microstructure of compacted graphite iron. *Journal of Materials Engineering and Performance*. 28(7), 3894-3904. DOI: 10.1007/s11665-019-03932-4
- [17] Hawryluk, M. & Mrzygłód, B. (2017). A durability analysis of forging tools for different operating conditions with application of a decision support system based on artificial neural networks (ANN). *Maintenance and Reliability*. 19(3), 338-348. DOI:10.17531/ein.2017.3.4
- [18] Han, Y., Qiao, G., Sun, J. & Zou, D. (2013). A comparative study on constitutive relationship of as-cast 904L austenitic stainless steel during hot deformation based on Arrhenius-type and artificial neural network models. *Science, Computational Materials*. 67, 93-103. DOI:10.1016/j.commatsci.2012.07.028
- [19] Yonghua, D., Lishi, M., Huarong, Q., Runyue, L. & Ping, J. (2017). Developed constitutive models, processing maps and microstructural evolution of Pb-Mg-10Al-0.5B alloy. *Materials Characterization*. 129, 353-366.
- [20] Reddy, N., You, H.L., Chan, H.P. & Chong, S.L. (2008). Prediction of flow stress in Ti-6Al-4V alloy with an equiaxed microstructure by artificial neural networks. *Materials Science and Engineering A*. 492(1-2), 276-282. DOI: 10.1016/j.msea.2008.03.030
- [21] Jingwei, J., Hua, D., Wenjuan, Z., Mingli, H., Dongbin, W. & Zhengyi, J. (2014). Modelling of the hot deformation behaviour of a titanium alloy using constitutive equations and artificial neural network. *Computational Materials Science*. 92, 47-56. DOI:10.1016/j.commatsci.2014.05.040
- [22] Lakshmi, A.A. Rao, C.S., Srikanth, M., Faisal, K., Fayaz, K. & Puspallatha, D. (2017). Prediction of mechanical properties of ASS 304 in superplastic region using artificial neural networks. *Materials Today: Proceedings*. 5(2), 3704-3712.
- [23] Vafaenezhad, H., Seyedein, S. & Aboutalebi, M. (2017). Application of constitutive description and integrated ANFIS - ICA analysis to predict hot deformation behavior of Sn-5Sb lead-free. *Journal of Alloys and Compounds*. 697, 287-299. DOI: 10.1016/j.jallcom.2016.12.148
- [24] Jia, W., Zeng, W., Han, Y., Liu, J., Zhou, Y. & Wang, Q. (2011). Prediction of flow stress in isothermal compression of Ti60 alloy using an adaptive network-based fuzzy inference system. *Materials & Design*. 32(10), 4676-4683. DOI: 10.1016/j.matdes.2011.06.053
- [25] Chunlei, G. & Mengjun, W. (2012). An application of ANFIS to predict the hot flow behavior of 6063 aluminum alloy. *Journal of Materials Engineering and Performance*. 21, 1160-1166. DOI: 10.1007/s11665-011-0033-y
- [26] Han, Y., Zeng, W. & Zhao, Y. (2011). An ANFIS model for the prediction of flow stress of Ti600 alloy during hot deformation process. *Computational Materials Science*. 50(7), 2273-2279. DOI:10.1016/j.commatsci.2011.03.004
- [27] Chen, D.-D., Lin, Y.C., Zhou, Y. & Chen, M.-S. (2017). Dislocation substructures evolution and an adaptive-network-based fuzzy inference system model for constitutive behavior of a Ni-based superalloy during hot deformation. *Journal of Alloys and Compounds*. 708, 938-946. DOI: 10.1016/j.jallcom.2017.03.029
- [28] Jonas, J., Sellars, C. & Mc Tegart, W. (1969). Strength and structure under hot-working conditions. *International Materials Reviews*. 14, 1-24. <https://doi.org/10.1179/mtrl.1969.14.1.1>
- [29] Lin, Y.C., Ming-Song, C. & Zhong, J. (2008). Constitutive modeling for elevated temperature flow behavior of 42CrMo steel. *Computational Materials Science*. 42(3), 470-477. <https://doi.org/10.1016/j.commatsci.2007.08.011>

- [30] Zhou, Y., Xiao-Min, C. & Qin, S. (2019). A strain-compensated constitutive model for describing the hot compressive deformation behaviors of an aged inconel 718 superalloy. *High Temperature Materials and Processes*. 38, 436-443. DOI:10.1515/htmp-2018-0108
- [31] Mahalle, G., Kotkunde, N., Gupt, A.K., Sujit, R., Kumar Sing, S. & Lin, Y. (2019). Microstructure characteristics and comparative analysis of constitutive models for flow stress prediction of inconel 718 alloy. *Journal of Materials Engineering and Performance*. 28(6), 3320-3331. DOI:10.1007/s11665-019-04116-w
- [32] Sabokpa, O., Zarei-Hanzaki, A., Abedi H. & Haghdadi, N. (2012). Artificial neural network modeling to predict the high temperature flow behavior of an AZ81 magnesium alloy. *Materials & Design*. 39, 390-396. DOI:10.1016/j.matdes.2012.03.002
- [33] Lin, Y.C., Hui, Y., He, D.-G. & Chen, J. (2019). A physically-based model considering dislocation-solute atom dynamic interactions for a nickel-based superalloy at intermediate temperatures. *Materials & Design*. 183, 108122. DOI: 10.1016/j.matdes.2019.108122
- [34] Lin, Y.C., Li, J., Chen, M.-S., Liu, Y.-X. & Liang, Y.-J. (2018). A deep belief network to predict the hot deformation behavior of a Ni-based superalloy. *Neural Comput & Applic*. 29, 1015-1023. <https://doi.org/10.1007/s00521-016-2635-7>
- [35] Manohar, M., Selvaraj, T., Sivakumar, D., Jeyapaul, R. & Jomy, J. (2014). Application of experimental design and analysis of mathematical models for turning inconel 718 using coated carbide tools. *Society for Experimental Mechanics*. 38, 61-71. <https://doi.org/10.1111/j.1747-1567.2012.00833.x>
- [36] Takagi T. & Sugeno, M. (1985). Fuzzy identification of systems and its applications to modelling and control. *IEEE Transactions on Systems, Man, and Cybernetics*. 15(1), 116-132.
- [37] Jang, J. (1993). ANFIS: adaptive-network-based fuzzy inference systems. *IEEE Transactions Systems Man Cybernetics*. 3, 665-685. DOI:10.1109/21.256541
- [38] Lin, Y., Li, K.-K., Li, H.-B., Chen, J., Chen, X.-M. & Wen, D.-X. (2015). New constitutive model for high-temperature deformation behaviour of inconel 718 superalloy. *Materials & Design*. 74, 108-118. <http://dx.doi.org/10.1016/j.matdes.2015.03.001>
- [39] Tan, Y., Ma, Y. & Zhao, F. (2018). Hot deformation behavior and constitutive modeling of fine grained Inconel 718 superalloy. *Journal of Alloys and Compounds*. 741, 85-96. <https://doi.org/10.3390/met8100846>
- [40] Sui, F., Xu, L., Chen, L. & Liu, X. (2011). Processing map for hot working of Inconel 718 alloy. *Journal of Materials Processing Technology*. 211(3), 433-440. DOI:10.1016/j.jmatprotec.2010.10.015
- [41] He, D.-G. Lin, Y., Jiang, X.-Y., Yin, L.-X., Wang, L.-H. & Wu, Q. (2018). Dissolution mechanisms and kinetics of δ phase in an aged Ni-based superalloy in hot deformation process. *Materials & Design*. 156, 262-271. DOI:10.1016/j.matdes.2018.06.058